17th World Conference on Earthquake Engineering, 17WCEE
Sendai, Japan - September 13th to 18th 2020

EXPERIMENTAL STUDIES ON A NEW ISOLATOR FOR BUILDINGS NEAR METRO TRANSPORTATION AND IN SEISMIC AREAS

T. Sheng (1), G.B. Liu (2), W.X. Shi (3), Y. Zhou(4)

(1) *Associate Professor, Department of Civil engineering, Ningbo University, China. shengtao@nbu.edu.cn*
(2) *Professor, Department of Civil engineering, Ningbo University, China. liuganbin@nbu.edu.cn*
(3) *Professor, Department of Disaster Mitigation for Structures, Tongji University, China. swxtgk@126.com*
(4) *Senior Engineer, Department of Civil engineering, Ningbo University, zhouye@nbu.edu.cn*

Abstract

Recent studies indicated that stacked sandbags can be used as an vertical isolator to reduce building vibrations caused by metro transportation. However, the bearing capacity of stacked sandbags is low, and the vertical stiffness is hard to be adjusted. Moreover, the ultimate shear deformation of stacked sandbags is too small to resist seismic vibrations. In order to overcome the above deficiencies, this paper presents a new kind of isolator for the buildings near metro transportation and in seismic areas. The isolator is composed of a laminated rubber bearing and particle mixture, and the particle mixture is composed of sand and rubber particles. There are some vertical through holes inside the rubber bearing, and the particle mixture is filled in the through holes. The results of compressive load tests showed that the vertical stiffness and the vertical damping ratio can be easily adjusted by changing the mixture ratio of the particle mixture. Compression-shear testing results showed that the internal friction forces between sand and rubber particles are a benefit to increasing the horizontal stiffness and the horizontal damping ratio, making the new isolator equal to a high-damping rubber bearing. The ultimate shear deformation of the new isolator exceeded 0.55 times of the effective diameter and 3 times of the total thickness of all rubber layers, proving that the new isolator is able to ensure the safety of a building under rare earthquakes. Furthermore, a field experiment with a full-scale building was performed to investigate the vibration suppression effectiveness of the new isolator. Testing results showed that the vertical vibration and secondary air-borne noise satisfied the limited value of human comfort after the installation of new isolators. It concluded that the new isolator is feasible for buildings near metro transportation and in seismic areas.

Keywords: Metro transportation; seismic area; laminated rubber bearing; particle mixture; compression-shear test; field experiment.

1. Introduction

Because of the punctuality, convenience and low pollution of metro transportation, a large number of metro lines have been constructed and are under construction all over the world. Especially in China, metro network construction has been the critical investment area designated by the country since 2006. According to the development plan of the national transportation of China, the total mileage of metro lines will reach 6000 km by the end of 2020. However, the vertical vibrations induced by such transportation lead to a comfort problem for residents inside the adjacent buildings. In order to solve the vibration problem, there are three kinds of ways: source reduction methods [1-2], wave barriers in the ground [3-4] and passive isolation methods of buildings [5-6].

Base isolation method with vertical isolators is one of the passive isolation methods. This method has been proved to be one of the most effective ways by Talbot [7], Sheng et al. [8] and many other researchers [9-10]. Since the strict requirements for vibration isolation and bearing capacity, the conventional vertical isolators for buildings near metro transportation are much more complicated and expensive right now. Moreover, there are even several defects for the conventional isolators.

For example, the bearing capacity of the steel spring isolator [9] is so small that only appropriate for light weight building. Furthermore, the steel material struggles to resist corrosion under humid conditions.

An elastomeric isolator with thickened rubber layers is another kind of vertical isolator for buildings near metro transportation [8, 10]. Although the bearing capacity of this isolator is high, it is hard to produce because the vertical stiffness values of different isolators are highly discrete, and it is impossible to adjust the values after the isolators are produced. Moreover, if the buildings near metro transportation locate in seismic areas at the same time, the base isolation method should also be designed to suppress the horizontal seismic vibrations. However, the above thick rubber isolator cannot resist earthquake vibrations because the ultimate shear deformation is dramatically reduced. Stacked sandbags are proved to be effective for suppressing metro-induced vertical vibrations of a building [11], but the ultimate shear deformation of the isolator is also limited and the bearing capacity is small [12-13]. Furthermore, it is also hard to adjust the vertical stiffness and the damping ratio of stacked sandbags.

So, some more reliable isolators should be deeply developed for the buildings near metro transportation and in seismic areas. This paper presents a new isolator to eliminate the disadvantages of conventional isolators, and meet the multiple requirements of the base isolation method. The mechanical properties and seismic isolation performances of the new isolator were tested in a lab first. Then, with a full-scale building near an existed metro line, a systematic field experiment was performed to investigate the suppression effectiveness of the new isolator for metro-induced vibration and noise.

2. The new isolator and mechanical tests

2.1 Design of the new isolator

The vertical and horizontal cross-sections of the new isolator are depicted in Figure 1 (a) and (b). The photos of a new isolator are shown in Figure 1 (c) and (d). At the top of the isolator, there is an enclosed space which is similar to a sandbag. The other part of the new isolator is an elastomeric seismic-protection isolator with some vertical through holes.

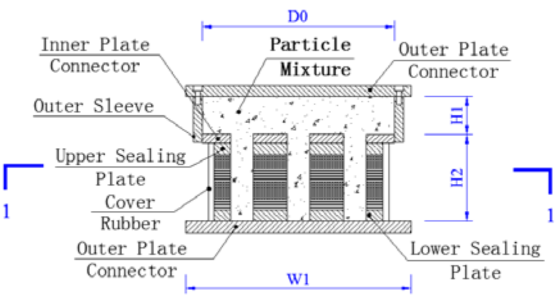

(a) Vertical cross-section.

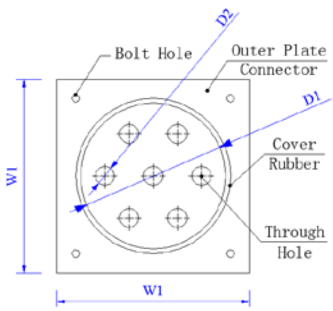

(b) Cross-section 1-1.

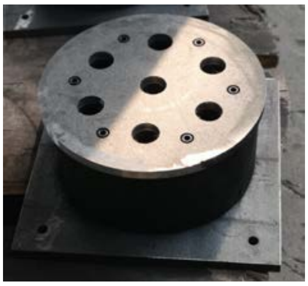

(c) The photo of the cross-section 1-1.

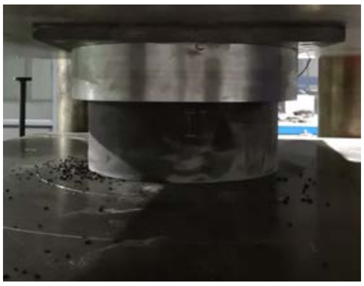

(d) The photo of the outer elevation.

Fig. 1 – Cross sections and photos of the new isolator.

Different from stacked sandbags, the new isolator is filled with particle mixture of sand and rubber particles. The sand particles are used to dissipate vertical kinetic energy by internal friction forces. The rubber particles are used to reduce the vertical stiffness of the isolator. By changing the mixture ratio of the particle mixture, vertical stiffness and damping ratio may be easily adjusted.

The particle mixture is also filled in the vertical through holes. As the compression stresses are concentrated on the vertical through holes, it is predicted that the holes are a benefit to further reducing the vertical stiffness of the isolator. Furthermore, the horizontal internal friction forces inside the through holes are theoretically a benefit to dissipating horizontal kinetic energy. The internal friction forces are expected to be an energy-dissipating component like lead core of an elastomeric isolator.

By increasing the diameter value of the new isolator, the section areas of the through holes is compensated. This means that the horizontal mechanical performances of the new isolator may be similar to those of a conventional elastomeric isolator. So the new isolator may be appropriate for the buildings near metro transportation and in seismic areas.

2.2 Tests for vertical mechanical properties

In order to verify the vertical mechanical properties of the new isolator, compression load tests were carried out. The vertical mechanical properties of an elastomeric isolator include compression stiffness and equivalent damping ratio. Table 1 lists four test conditions of the compression load tests. The mixture ratios of the particle mixture gradually change under different conditions.

Table 1 – Test conditions of the compression load tests.

Test conditions		1	2	3	4
Mixture ratios	**Sand**	100%	50%	0%	0%
	Rubber	0%	50%	100%	0%

Before compression load tests, three cycles of pre-compression were processed to ensure the compaction of the new isolator. Then, in order to test the hysteresis loops, the isolator were cyclically loaded and unloaded between 0 MPa and 1.3 times of the design compression stress. The vertical pseudo-static loading method is similarly to that proposed by Liu et al.[14].

2.3 Tests for horizontal mechanical properties

In order to verify the horizontal mechanical properties of the new isolator, compression-shear load tests were carried out. The horizontal mechanical properties including equivalent shear stiffness and equivalent damping ratio are obtained from tested hysteresis loops [15].

According to the standard of ISO 22762-1 [16], there are at least three items should be tested for a new isolator: (1) compression stress dependency, (2) shear strain dependency, and (3) ultimate shear deformation. Since the mixture ratio of the particle mixture is an important factor, the mixture ratio dependency of the new isolator is also tested. The test conditions are listed in Table 2.

Table 2 – Test conditions of the compression-shear load tests.

No.	**Test items**	**Fixed parameter**	**Variable parameter**
1	Compressive stress (σ_V) dependency.	(1) γ = 100%. (2) Sand: 50%, and rubber: 50%.	σ_V = 2 MPa
2			σ_V = 5 MPa
3			σ_V = 7 MPa
4			σ_V = 10 MPa

5	Shear strain (γ) dependency.	(1) σ_V = 10 MPa. (2) Sand: 50%, and rubber: 50%.	γ = 100%
6			γ = 175%
7			γ = 250%
8	Mixture ratio dependency.	(1) γ = 100%. (2) σ_V = 5 MPa.	Condition 1 of Table 1.
9			Condition 2 of Table 1.
10			Condition 3 of Table 1.
11			Condition 4 of Table 1.
12	Ultimate shear deformation.	The same as condition 7.	γ = max (0.55D, 300%)

As required by the seismic code of China [17], the ultimate shear deformation of an elastomeric isolator, under compressive stress of 10 MPa, should exceed 0.55 times of the isolator's effective diameter or 3 times of the total thickness of all rubber layers.

A new isolator with dimensions shown in Table 3 was produced for the above tests. There are 20 inner rubber layers and 19 inner steel plates inside the elastomeric isolator. The thickness of a single rubber layer is 3 mm, and the thickness of a single steel plate is 2 mm. The distance between two adjacent through holes is about 100 mm. A compression-shear testing machine which fits the accuracy requirements of ISO 22762-1 [16] was selected in the above tests. Testing photos of the new isolator are shown in Figure 2.

Table 3 – Dimensions of a new isolator.

Dimensions	D0	D1	D2	W1	H1	H2
Values / mm	345	300	40	400	66	154

(a) Compression load test.

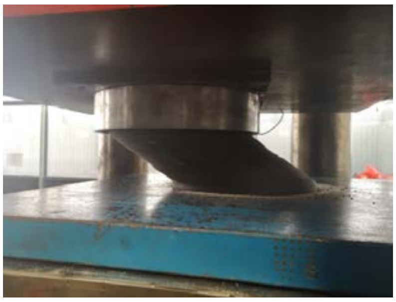

(b) Compression-shear load test.

Fig. 2 – Testing photos of the new isolator.

3. Mechanical testing results and analysis

3.1 Vertical mechanical properties

The tested hysteresis loops of the conditions listed in Table 1 are illustrated in Figure 3. As metro induced environmental vibrations are micro amplitude waves, the vertical stiffness values are derived from the tangent stiffness values. As shown in Figure 3, the tangent stiffness values located at 10 MPa is close to the secant stiffness values from 8 MPa to 12 MPa, so the secant stiffness values are also appropriate for the isolators. The equivalent damping ratios in Figure 3 are deduced regarding hysteresis loops based on energy conservation principle [18]. Table 4 lists the tested results of the vertical stiffness values and the vertical damping ratios.

The vertical stiffness values in Figure 3 (a), (b) and (c) increase when the pressure force increases. This is because the particle mixture becomes more and more dense at that case, and rubber particles have a special characteristic of hardening stiffness. In addition, the more the sand particles are included, the larger the hysteresis loop areas are, proving sand particles are able to dissipate kinetic energy as expected.

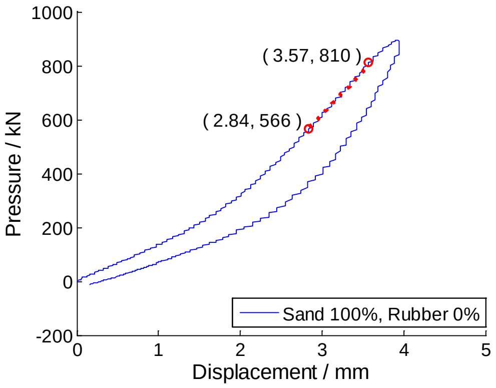

(a) Condition 1.

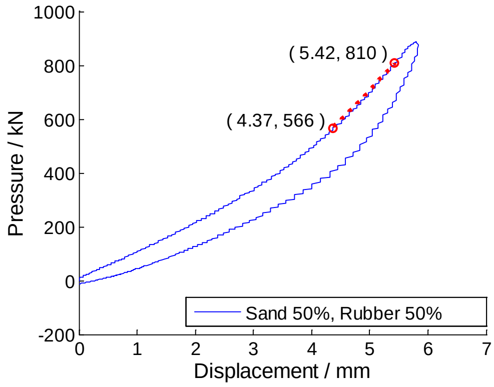

(b) Condition 2.

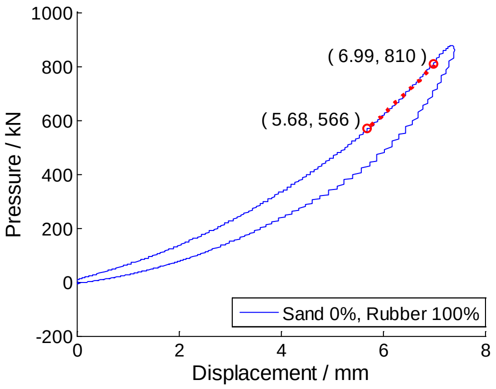

(c) Condition 3.

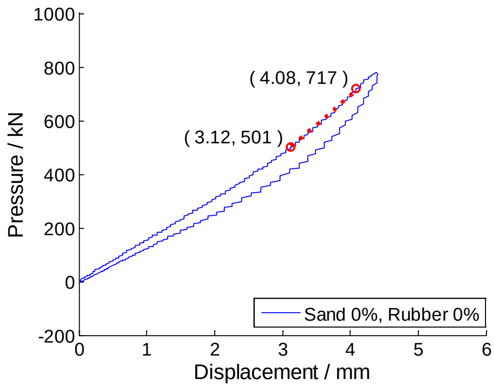

(d) Condition 4.

Fig. 3 – Tested hysteresis loops of the conditions listed in Table 1.

Table 4 – Testing results of the new isolator.

Conditions	1	2	3	4
Vertical stiffness / kN/mm	213.5	140.1	107.9	168.4
Equivalent damping ratio	9.0%	8.3%	6.8%	4.2%

As shown in Table 4, the vertical stiffness value of the isolator under condition 4 is much smaller than that of condition 1, proving that the sand particles filled in the isolator are able to increase the vertical stiffness. Nevertheless, the vertical stiffness value of condition 1 is 1.66 times more than that of condition 2, and 2 times more than that of condition 3. This phenomenon proves that rubber particles filled in the isolator are effective to reduce the vertical stiffness.

Since the isolator of condition 4 is without any particle mixture, the hysteresis loop area shown in Figure 3 (d) is the smallest, the damping ratio listed in Table 4 is also the smallest. For the isolator of condition 1 which is only filled with sand particles, the vertical damping ratio is the largest and the isolator equals to a high damping rubber bearing. For the isolator of condition 3 which is only filled with rubber particles, the damping ratio is also much larger than that of condition 4.

It concluded that the particle mixture is effective to adjust the vertical stiffness and the damping ratio, and the adjusting way is very easy and economical.

3.2 Horizontal mechanical properties

The tested hysteresis loops of the first four conditions in Table 2 are illustrated in Figure 4 (a). The loops are full, and the hysteretic performances are good. The deduced shear stiffness values and the horizontal equivalent damping ratios are illustrated in Figure 4 (b).

According to the design theories on the compression stress dependency [15], the shear stiffness of a conventional elastomeric isolator decreases when the compression stress increases. However, for the new isolator, the shear stiffness value shown in Figure 4 (b) increases firstly and then slowly decreases when the compression stress increases from 2 MPa to 10 MPa. This is because the internal friction forces inside the through holes simultaneously increases at that case. So, it concluded that the particle mixture is a benefit to increasing the shear stiffness and ensuring the stability.

As shown in Figure 4 (b), the horizontal damping ratios are between 19% and 36%, proving that the internal friction forces inside the vertical through holes are a benefit to dissipating horizontal kinetic energy as expected. So, the particle mixture equals to an energy-dissipating component, and the new isolator equals to a high-damping rubber bearing in horizontal direction.

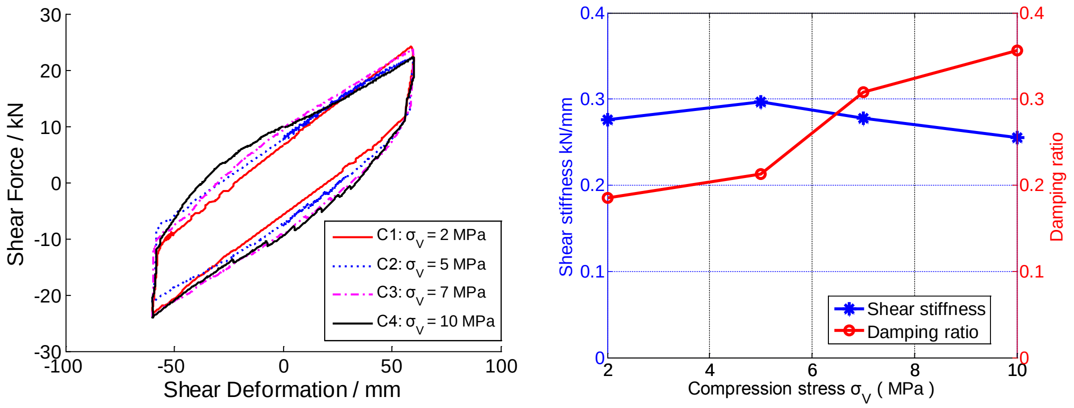

(a) Tested hysteresis loops. (b) Shear stiffness and damping ratio.

Fig. 4. Compressive stress dependency.

For the condition 5, the condition 6 and the condition 7 listed in Table 2, the tested hysteresis loops are illustrated in Figure 5 (a). The loops are also very full, and the hysteretic performances are also good. The deduced shear stiffness values and the equivalent damping ratios are illustrated in Figure 5 (b).

According to the design theories on the shear strain dependency [15], the shear stiffness value of a conventional elastomeric isolator decreases when the compression stress increases. For the new isolator, the shear stiffness value shown in Figure 5 decreases by 55 percent when the shear strain increases from 100% to 250%, which is same as a conventional elastomeric isolator. Because the kinetic energy dissipated by internal friction forces increases when the shear strain increases, and the shear stiffness decreases at the same time, the equivalent damping ratio shown in Figure 5(b) increases from 18% to 60%. This phenomenon proves that the new isolator is more appropriate for resisting rear earthquakes.

For the condition 8, the condition 9, the condition 10, and the condition 11, the tested hysteresis loops are illustrated in Figure 6 (a). The force-deformation curves of condition 12 is depicted in Figure 6 (b). Table 5 lists the tested shear stiffness values and the equivalent damping ratios of these conditions.

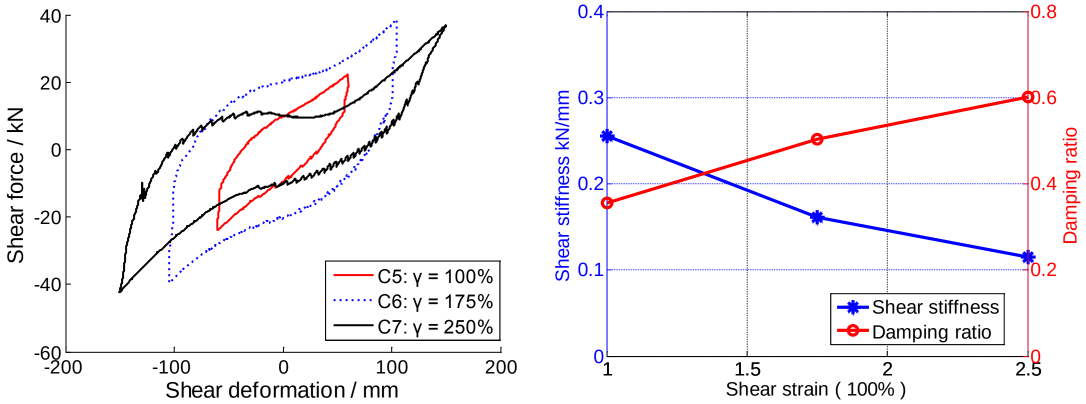

(a) Tested hysteresis loops. (b) Shear stiffness and damping ratio.

Fig. 5. Shear strain dependency.

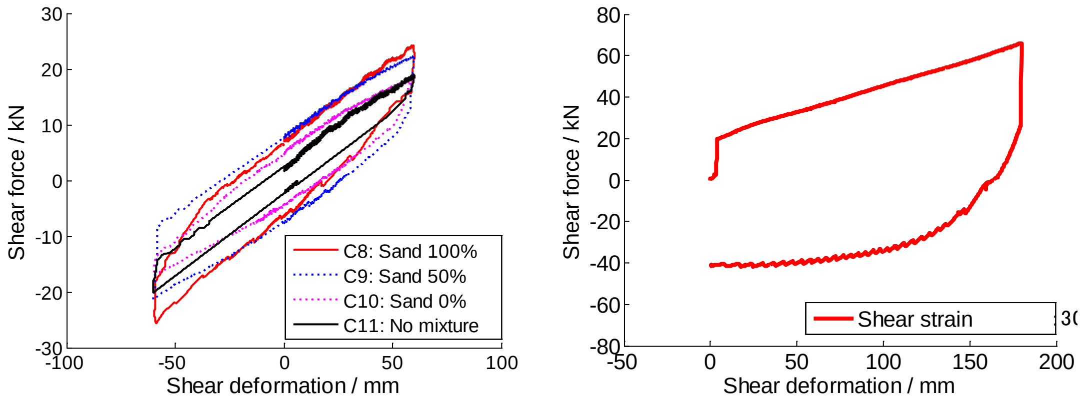

(a) Tested hysteresis loops. (b) Shear force-deformation curves.

Fig. 6. Mixture ratio dependency and the ultimate shear deformation.

Table 5 – Tested values of mixture ratio dependency.

Conditions	8	9	10	11
Vertical stiffness / kN/mm	0.359	0.297	0.283	0.266
Equivalent damping ratio	17.1%	21.3%	12.4%	6%

The test results in Figure 6 (a) show that the hysteresis loops of condition 8 and condition 9 are much fuller than the others, and the loop of condition 11 is the thinnest. As listed in Table 5, the shear stiffness of condition 8 is the largest, and the value of condition 11 is the smallest. The isolator of condition 8 is only filled sand particles, and the isolator of condition 11 is without any particle mixture. It concluded that the particle mixture is a benefit to increasing the shear stiffness, and the more the sand particles are included, the larger the shear stiffness value is.

Compared with condition 8, the shear stiffness and the strain energy of condition 9 dramatically reduced. As the reduction of friction forces of condition 9 is not as much as that of the strain energy, the equivalent damping ratio of condition 9 is the largest one in Table 5. The isolator of condition 11 equals to a low damping rubber bearing, and all the other isolators equal to high damping rubber bearings. This phenomenon proves that mixture ratio of the particle mixture has obvious influences on the horizontal internal friction forces.

For the new isolator, 3 times of the total thickness of all rubber layers is 180 mm, and 0.55 times of the isolator's effective diameter is 155 mm. The test results in Figure 6 (b) show that the ultimate shear deformation of the new isolator exceeds 180 mm, and therefore the new isolator is able to ensure the safety of a building under rear earthquakes.

4. Field experiments and analysis

A full-scale one-story masonry building was built near an existed metro trestle in Ningbo, China. Figure 7 (a) and (b) show the front elevation and the photo of the masonry building. In order to investigate the suppression effectiveness of the new isolator for vertical vibration and secondary air-borne noise, a systematic field experiment was operated. Figure 7(c) and (d) show the photos of the installed isolators and the measuring sensors. The installed isolators are only filled with rubber particles.

The dimensions of the building were 3.0×2.8×2.8 m, corresponding to length×width×height. The thickness of the floor slabs was 100 mm. As shown in Figure 7(a), a base isolation layer and a top ring beam were designed for the buildings, both of which were made of reinforced concrete. The natural frequency of the floor slab of the one-story building is identified as 80 Hz by knocking tests. After the installation of the new isolators, the isolation frequency is identified as 12.5 Hz, which is much lower than the natural frequency of the floor slab.

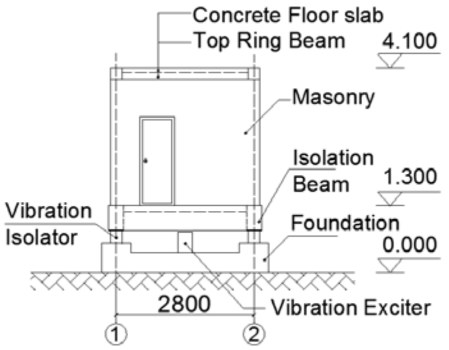

(a) The front elevation of the building.

(b) The photo of the building.

(c) The installed new isolator.

(d) The acceleration and sound pressure sensors.

Fig. 7. The field experiment with the full-scale building.

As recommended by the standards of ISO 2631-2 [19], frequency vibration levels (abbreviated as “frequency VLs”) and frequency A-weighted sound pressure levels (abbreviated as “frequency LAs”) were selected to evaluate the human comfort inside the building. Figure 8 (a) shows the averaged frequency VLs, and Figure 8 (b) shows the averaged frequency LAs. According to the standard of China [20], The limit values for human vibration and noise comfort in this paper are determined to be 67 dB and 38 dB respectively.

In Figure 8(a), the peak value of frequency VLs decreased by 14 dB. In Figure 8(b), the peak value of frequency LAs decreased by 10 dB. All of the values in Figure 8 satisfied the limit value of human comfort. The above results prove that the new isolator is effective to suppress the vertical vibrations and secondary air-borne noise caused by metro transportation.

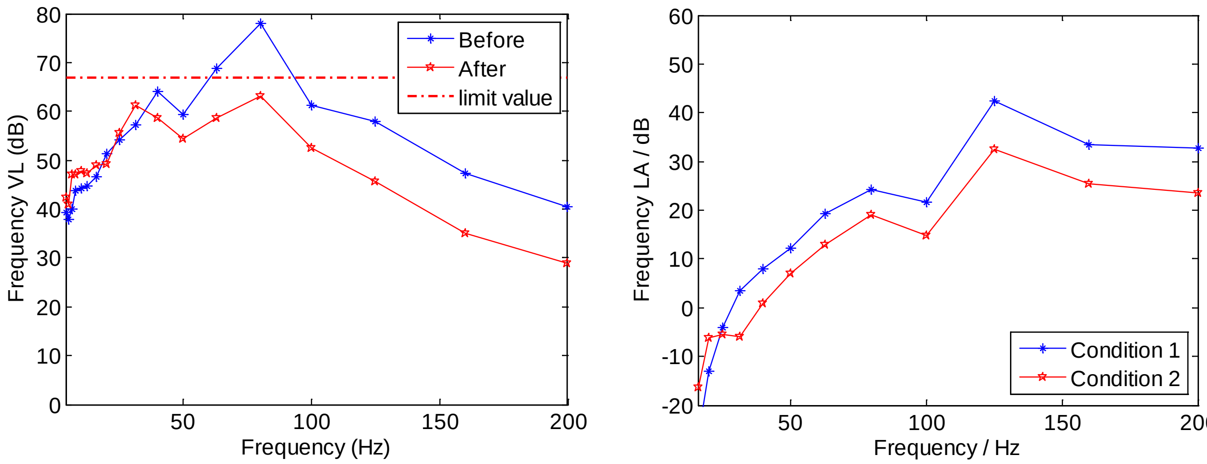

(a) Frequency vibration level. (b) Frequency A-weighted sound pressure level.

Fig. 8. Tested values of human comfort inside the building.

5. Conclusions

(1) Adjusting mixture ratio is an easy and economical way to adjust the vertical stiffness and the equivalent damping ratio of the new isolator. The more the sand particles are included, the larger the damping ratio is. The more the rubber particles are included, the lower the vertical stiffness is.

(2) The internal friction forces generated by sand and rubber particles are a benefit to increasing the horizontal stiffness and the stability of the new isolator. The shear stiffness dependency of the new isolator is same as that of a conventional elastomeric isolator. The new isolator equal to a high-damping rubber bearing. The larger the shear strain is, the larger the damping ratio is, and therefore the new isolator is more appropriate for resisting rear earthquakes.

(3) Mixture ratio influences the shear stiffness and the equivalent damping ratio of the new isolator. The more the sand particles are included in the isolator, the larger the shear stiffness is. The ultimate shear deformation of the isolator is able to ensure the safety of a building under rear earthquakes.

(4) The new isolator is able to enhance the comfort for residents inside buildings near metro transportation. After the installation of the new isolators, the frequency vibration levels and the frequency A-weighted sound pressure levels inside the building were suppressed by 14 dB and 10 dB respectively.

It concluded that the mechanical performances of the new isolator satisfy the vibration control requirements of the building near metro transportation and in seismic areas. The structure of the new isolator is simple, and therefore it has a positive application value in practical engineering.

6. Acknowledgements

This work was supported by the Natural Science Foundation of Zhejiang province, China (Grant Nos. LY18E080011); the Ningbo Natural Science Foundation (Grant Nos. 2019A610402).

7. Copyrights

17WCEE-IAEE 2020 reserves the copyright for the published proceedings. Authors will have the right to use content of the published paper in part or in full for their own work. Authors who use previously published data and illustrations must acknowledge the source in the figure captions.

8. References

[1] Lombaert G, Degrande G, Vanhauwere B (2006): The control of ground-borne vibrations from railway traffic by means of continuous floating slabs. *Journal of Sound and Vibration*, 297, 946-961.

[2] Sheng T, Zhang SL, Shan JZ, Shi WX (2015): In-situ measurement and analysis of subway-induced environmental vibration and the effectiveness of vibration-source suppression methods. *Journal of Vibration, Measurement and Diagnosis*, 35 (2), 352-358 (in Chinese).

[3] Coulier P, Cuéllar V, Degrande G, Lombaert G (2015): Experimental and numerical evaluation of the effectiveness of a stiff wave barrier in the soil. *Soil Dynamics and Earthquake Engineering*, 77, 238-253.

[4] Yang Y, Ge P, Li Q, Liang X, Wu Y (2018): 2.5D vibration of railway-side buildings mitigated by open or infilled trenches considering rail irregularity. *Soil Dynamics and Earthquake Engineering*, 106, 204-214.

[5] Newland DE, Hunt HEM (1991): Isolation of buildings from ground vibration: a review of recent progress. *Mechanical Engineering Science*, 205 (l), 39-52.

[6] Cho T (2013): Experimental and numerical analysis of floating floor resonance and its effect on impact sound transmission. *Journal of Sound and Vibration*, 332 (25), 6552-6561.

[7] Talbot JP, Hunt HEM (2003): Isolation of buildings from rail-tunnel vibration: a review. *Building Acoustics*, 10(3), 177-192.

[8] Sheng T, Li YM, Zhang H, Shi WX, Yang Y (2015): Field experiment study of subway nearby building's base isolation by laminated thick rubber isolator. *Journal of Building Structures*, 36(2), 35-40 (in Chinese) .

[9] Wagner H (2004): Vibration control systems for trackbeds and buildings using coil steel springs. *Proceedings of acoustics*, Gold Coast, Australia.

[10] Pan P, Shen S, Shen Z, Gong R (2018): Experimental investigation on the effectiveness of laminated rubber bearings to isolate metro generated vibration. *Measurements*, 122, 554-562.

[11] Sheng T, Li SM, Liu GB, Hou SS, Wang JC (2017): Tests for subway nearby building's base vibration isolation with sandbag layers. *Journal of Vibration and Shock*, 36(2): 35-40 (in Chinese).

[12] Liu SH, Gao JJ, Wang YQ (2014): Experimental study on vibration reduction by using soilbags. *Geotextiles and Geomembranes*, 42(1), 52-62.

[13] Sheng T, Xiao C, Li SM, Jin HL (2018): Test for vertical bearing performance of sandbag layer. *Industrial Construction*, 48(6), 96-184 (in Chinese).

[14] Liu JF, Xie HP, Xu J (2008): Experimental study on damping characteristics of rock under cyclic loading. *China Journal of Rock Mechanics and Engineering*, 27(4), 712-717 (in Chinese).

[15] Architecture Institute of Japan (2016): *Design recommendations for seismically isolated buildings*, 4th edition (in Japanese).

[16] ISO22762-1 (2005): *Elastomeric seismic-protection isolators - Part 1: Test methods.*

[17] MOHURD of the P.R. China (2010). *Code for seismic design of buildings*. China Architecture and Building Press, Beijing (in Chinese).

[18] Hardin BO, Drnevich VP (1972). Shear modulus and damping in soil: design equations and curves. *Journal of Soil Mechanicals - Foundation Division, ASCE*, 98(7), 667-692.

[19] ISO2631-2 (2003): *Mechanical vibration and shock-Evaluation of human exposure to whole-body vibration - Part 2: Vibration in buildings (1 Hz to 80 Hz).*

[20] MOHURD of the P.R. China (2009). *Standard for limit and measuring method of building vibration and secondary noise caused by urban rail transit*. Beijing, China architecture & building press, 2009 (in Chinese).

